A role for worm *cutl-24* in background- and parent-of-origin-dependent ER stress resistance

Wenke Wang[1,2], Anna G. Flury[1,2], Jennifer L. Garrison[1,3,4]*, and Rachel B. Brem[1,2,3]*

[1]Buck Institute for Research on Aging, Novato, CA

[2]Department of Plant and Microbial Biology, UC Berkeley, Berkeley, CA

[3]Leonard Davis School of Gerontology, University of Southern California, Los Angeles, CA

[4]Department of Cellular and Molecular Pharmacology, UC San Francisco, San Francisco, CA; Global Consortium for Reproductive Longevity & Equality, Novato, CA

*Authors for correspondence: jgarrison@buckinstitute.org, rbrem@berkeley.edu.

Abstract

Organisms in the wild can acquire disease and stress resistance traits that far outstrip the programs endogenous to humans. Finding the molecular basis of such natural resistance characters is a key goal of evolutionary genetics. Standard statistical-genetic methods toward this end can perform poorly in organismal systems that lack high rates of meiotic recombination, like *Caenorhabditis* worms. Here we discovered unique ER stress resistance in a Kenyan *C. elegans* isolate, which in inter-strain crosses was passed by hermaphrodite mothers to hybrid offspring. We developed an unbiased version of the reciprocal hemizygosity test, RH-seq, to explore the genetics of this parent-of-origin-dependent phenotype. Among top-scoring gene candidates from a partial-coverage RH-seq screen, we focused on the neuronally-expressed, cuticlin-like gene *cutl-24* for validation. In gene disruption and controlled crossing experiments, we found that *cutl-24* was required in Kenyan hermaphrodite mothers for ER stress tolerance in their inter-strain hybrid offspring, and was a contributor to the trait in their purebred progeny. These data establish the Kenyan strain allele of *cutl-24* as a determinant of a natural stress-resistant state, and they set a precedent for the dissection of natural trait diversity in invertebrate animals without the need for a panel of meiotic recombinants.

Introduction

Understanding mechanisms of trait diversity in organisms from the wild is a central goal of modern genetics. Classical methods toward this end, namely association and linkage mapping, have enabled landmark successes in the field (Flint and Mott 2001). These tools are well-suited to organismal systems in which highly polymorphic, well-mixed recombinant populations exist in the wild or can be generated in the lab. Such features are lacking in the nematode worm *Caenorhabditis.* The laboratory strain of *C. elegans* has been a fixture of the biology literature for decades (Nigon and Félix 2017), but dissecting natural variation in nematodes has proven to be a challenge owing to low rates of polymorphism and meiotic recombination (Hillers and Villeneuve 2003). In a few model *C. elegans* systems, landmark resources have been established to overcome these limitations (Li *et al.* 2006; Reddy *et al.* 2009; Rockman and Kruglyak 2009; McGrath *et al.* 2009; Doroszuk *et al.* 2009; Seidel *et al.* 2011; Bendesky *et al.* 2012; Ghosh *et al.* 2012, 2015; Balla *et al.* 2015; Andersen *et al.* 2015; Large *et al.* 2016; Ben-David *et al.* 2017), including recent progress with genome-wide association scans (Webster *et al.* 2019a; Na *et al.* 2020; Evansid *et al.* 2021). Despite these advances, the power of natural variation genetics remains out of reach for many nematode strains and species.

The reciprocal hemizygosity test (Stern 2014) is a strategy to map genotype to phenotype that complements linkage and association approaches. This approach starts with an F1 hybrid formed from the mating of two genetically distinct lines of interest. An induced mutation in the hybrid at a given gene disrupts the allele from each parent in turn, uncovering the other allele in a hemizygous state. The set of hemizygote mutants allow a comparison of phenotypes conferred by the two parents' alleles, controlled for background and ploidy. Strengths of the method include the ability for trait dissection without a panel of meiotic recombinants, and the potential for genetic insights into traits unique to hybrid backgrounds (heterosis, for example, and imprinting and other parent-of-origin effects; Comings and MacMurray 2000; Reinhold 2002;

Wolf and Wade 2009; Timberlake 2013; Monk *et al.* 2019)). Our group previously established genome-wide reciprocal hemizygosity mapping in yeast (RH-seq; (Weiss *et al.* 2018)), and we reasoned that nematodes could serve as a useful testbed for an extension of the method to multicellular animals.

For a case study using RH-seq, we set out to identify natural stress resistance states in wild worms, and to probe their genetics. We chose to focus on ER protein folding quality control, which is essential in eukaryotes for development and stress response, and is a linchpin of diabetes, neurodegenerative disease, and other human disorders (Hebert and Molinari 2007; Roth *et al.* 2010). Surveying *C. elegans* isolates, we characterized a Kenyan strain with a ER stress resistance phenotype, and we discovered a robust parent-of-origin effect in hybrids derived from this strain. To enable the search for determinants of this trait variation, we developed an implementation of RH-seq for the worm which achieved unbiased, partial coverage of the genome. From the results we focused on one gene hit, *cutl-24*, for validation of its impact on ER stress response.

Materials and Methods

Worm strains

Wild-type strains of *C. elegans* AB1 (Adelaide, Australia), CB4856 (Hawaii, USA), CB4932 (Taunton, Great Britain), ED3052 (Ceres, South Africa), ED3077 (Nairobi, Kenya), GXW1 (Wuhan, China), JU1088 (Kakegawa, Japan), JU1172 (Concepcion, Chile), JU1652 (Montevideo, Uruguay), JU262 (Indre, France), JU393 (Hermanville, France), JU779 (Lisbon, Portugal), MY16 (Munster, Northwest Germany), N2 (Bristol, Great Britain) and PX179 (Eugene, USA) were used in this study, all from the *Caenorhabditis* Genetics Center.

Tunicamycin resistance assays

Tunicamycin resistance assays were performed as described (Henis-Korenblit *et al.* 2010) with modifications as follows. For Figure 1, 2-3 day 1 gravid adults of different strains were placed onto plates containing 5 µg/mL tunicamycin (InSolution, Sigma) which was added to NGM media before pouring and allowed to lay eggs for 12 hours. The number of eggs was counted (typically 50-200) and compared with the number of animals that reached the adult stage within 96 hours at 20°C. In controls on untreated (DMSO) plates, ~100% of eggs hatched for a given strain. For each bar in Figure 2, 5-10 L4 hermaphrodites of the indicated strain were incubated with 10-20 males of the indicated strain for 24 hours to allow mating. The hermaphrodites were then transferred onto plates containing 5 µg/mL tunicamycin (InSolution, Sigma) as above and allowed to lay eggs for 12 hours. The proportion of eggs from the indicated cross that developed to adulthood in the presence of tunicamycin was calculated the same as in Figure 1 and was normalized to the analogous quantity from wild-type ED3077. For Figure 5, the experimental condition was the same as above except 10 µg/mL tunicamycin (InSolution, Sigma) was used and the number of animals that reached the adult stage was counted after 66-68 hours at 25°C.

RH-seq in *C. elegans*

RH-seq parental strain construction.

To enable the heat-induced Mos1 transposon system (Bessereau *et al.* 2001; Williams *et al.* 2005; Duverger *et al.* 2007) in the ED3077 and N2 backgrounds, we proceeded as follows.

For mutagenesis in N2, we used IG358 (oxEx229 [Mos1 Substrate + *myo-2p*::GFP]), an N2 transgenic which carries multiple copies of the Mos1 transposon and pharynx-specific green fluorescent protein (GFP) expression, and IG444 (frEx113 [(pJL44) transposase + *col-12p*::DsRed]), an N2 transgenic which carries the coding sequence of the Mos1 transposase under the control of a heat-shock promoter and a coelomocyte-specific DsRed reporter.

For the corresponding strains in the ED3077 background, we injected the pSM-Mos1 transposon plasmid at 25 ng/µl, pCFJ421 (P*eft-3::gfp::h2b*) at 10 ng/µl, and pSM at 65 ng/µl to yield ED3077-gG. We injected pJL44 (P*hsp16.48::MosTase::glh-2utr*) at 50 ng/µl, pCFJ90 (P*myo-2::mCherry::unc-54utr*) at 2 ng/µl, and pSM at 48ng/µl to create ED3077-3R.

After mutagenesis, to enable the collection of progeny from mutant hermaphrodites in one background mated to wild-type males from the other (see below), we used labeled strains for the latter. To make these, wild-type ED3077 and wild-type N2 were injected with pCFJ104 (P*myo-3::mCherry::unc-54utr*) and pCFJ90 (P*myo-2::mCherry::unc-54utr*) respectively at 5 ng/µl, after which the respective transgene was integrated into the worm genome by UV/TMP treatment. The worms were outcrossed 3 time.

RH-seq hemizygote construction and phenotyping

Our RH-seq workflow proceeded in 13 rounds in N2. For each round of hemizygotes bearing mutations in the N2 alleles of genes, we first made Mos1-ready N2 animals by picking 100-200 L4 hermaphrodites of IG358 and 200 L4 males of IG444 onto one NGM plate. After 12 hrs at 25°C, the hermaphrodites and males were transferred to a new NGM plate for egg-lay. 100-200 F1 progeny exhibiting GFP and mCherry marker expression (*i.e.*, containing both transposase and transposon arrays) were hand-picked at the L4 stage.

In these Mos1-ready N2 animals, we induced Mos1 transposition at the young adult stage by heat-shock treatment as described (34 °C for 1 h, 20 °C for 1 h and 34 °C for 1 h) (Boulin and Bessereau 2007). We collected the putatively mutant eggs and selfed them for two generations to ensure appreciable numbers of clones of a given mutant genotype. We collected 20,000-50,000 F3 progeny and sorted in a Union Biometrica COPAS Biosort for those that had lost the substrate array and transposase array (*i.e.,* they lacked GFP and mCherry expression) to prevent continued transposition for the rest of the experiment.

We transferred 10,000-20,000 of these putatively mutant N2 hermaphrodites to NGM plates with 5,000-10,000 labeled wild-type ED3077 males (see above) and allowed mating to occur for one and half day at 15°C. The mated hermaphrodites were lysed, and ~30,000 eggs were transferred to one plate (5-10 plates per round) containing 10 µg/mL tunicamycin, followed by incubation for development for 66-68 hrs at 25°C.

Afterward, 3,000-12,000 surviving worms were collected and sorted, with only hermaphrodite adults (assessed based on size) and hybrid progeny of the marked ED3077 parent (assessed based on mCherry marker expression) retained for DNA isolation and sequencing (see below).

11 rounds of hemizygotes bearing mutations in the ED3077 alleles of genes proceeded as above, except that we mated ED3077-gG with ED3077-3R to make Mos1-ready ED3077, and after mutagenesis, we mated the resulting putatively mutant hermaphrodites in the ED3077 background to mCherry-marked wild-type N2 males to yield hemizygotes.

Genomic DNA extraction from *C. elegans*

Animals from hemizygote pools that had been collected after control or tunicamycin treatment from a given RH-seq round were collected and snap-frozen in liquid nitrogen. Genomic DNA (gDNA) from the worm pellets were extracted using the DNeasy Blood & Tissue Kit (Qiagen) and a *C. elegans* gDNA extraction protocol from the Kaganovich lab (University Medical Center Göttingen, http://www.kaganovichlab.com/celegans.html). The purified gDNA was quantified using a Nanodrop.

Transposon insertion sequencing library construction

Illumina transposon sequencing libraries were constructed using the FS DNA Library Kit (NEB) as follows. By following the protocol, gDNA was enzymatically digested and ligated with E-adapters (a duplex whose upper strand is longer than the lower). The E-adapter upper arm was GGGCGTAGATTACCGTCCGCGACTCGTACTGTGGCGCGCC*T (*T indicates T overhang),

and the E-adapter lower arm was /Phos/GGCGCGCCACAGTACTTGACTGAGCTTTA/3ddC/. Sequences containing the 3' junction of each inserted Mos1 transposon to the genome were amplified using a Mos1 transposon primer (5'-AATGATACGGCGACCACCGAGATCTACACTCTTTCCCTACACGACGCTCTTCCGATCTNNNNNNXXXXXXGATTTAAAAAAAACGACATTTCATAC-3' N, random sequence; XXXXXX, barcode indices; GATTTAAAAAAAACGACATTTCATAC, Mos1 transposon sequences) and a primer homologous to a region of the adapter (CAAGCAGAAGACGGCATACGAGATACATCGGGGGCGTAGATTACCGTCCGCGACTC). The thermocycler protocol was as follows: 98°C for 30 seconds, (98°C for 10 seconds, 65°C for 1 minute and 15 seconds) x 24, 65°C for 10 minutes, 4°C hold. Single-end sequencing of 100 bp was then done on a NovaSeq machine at the Vincent J. Coates Genomics Sequencing Lab at the University of California, Berkeley. In total, we sequenced 22 libraries from pools of hemizygotes bearing mutations in the ED alleles of genes (representing one tunicamycin-treated and one untreated pool from each of 11 rounds), and 26 libraries from pools bearing mutations in the N2 alleles of genes (representing one tunicamycin-treated and one untreated pool from each of 13 rounds), generating 3-20 million reads per library (Table S3).

RH-seq read-mapping

For a given library of reads reporting transposon insertion sequencing from hemizygotes after tunicamycin or control treatment for RH-seq, we first removed adapter sequences from the end of the reads using fastx_clipper from the fastx toolkit. Then, using fastx_trimmer from the fastx toolkit, we removed the first 6 bp of every read, so every read would now begin with the barcode index sequence. We then demultiplexed the barcode indexes using the fastx_barcode_splitter from the fastx toolkit. Using an adapted custom python script, we retained for analysis only reads containing the last 28 bp of the Mos1 transposon, allowing for no mismatches. For this subset of reads containing the transposon, we excised the sequence immediately flanking the

end of the transposon sequence, and mapped the remainder of the read (containing the stretch of genome adjoining the transposon insertion) to the respective genome using BLAT (minimum sequence identity = 100; tile size= 12).

For pools of hemizygotes bearing transposon insertions in the N2 alleles of genes, we mapped to the N2 genome from BioProject PRJNA13758, release WS271. For hemizygotes with insertions in the ED3077 alleles, we mapped to a ED3077 reference genome made as follows. We downloaded raw genome sequencing reads for ED3077 from https://www.elegansvariation.org/ (Cook *et al.* 2017). These reads were aligned to genome assembly WS271 of the reference sequence of the *C. elegans* N2 strain using bowtie2 with default parameters. Samtools, bcftools, and bgzip were used to call SNPs, retaining those with a quality score of >20 and combined depth of >5 and <71. We then generated a pseudogenome by replacing the reference N2 allele with that of ED3077 at each SNP using bcftools.

We eliminated reads whose genomic sequence portion was shorter than 30 bp and/or mapped to more than one location in the genome. For analysis of a given sequencing library, we inferred that reads that mapped to genomic positions within 100 bp of each other originated from the same transposon mutant clone and assigned the sum of their counts to the position which had the most mapped reads. Then, for a given insertion in a given library, we considered the number of reads mapped to that position, n_{insert}, as the relative proportional abundance of the mutant in the worm pellet whose gDNA was sequenced. In order to compare abundances across samples and libraries, we divided n_{insert} by the total number of reads in the sample to get the normalized abundance.

RH-seq data analysis

We used N2 genome annotations from BioProject PRJNA13758, release WS271, to determine whether an inferred transposon insertion position was genic or non-coding, and we retained only those insertions which were genic. For a given insertion observed in sequencing from a given

RH-seq round (comprising a pool of hemizygotes split into tunicamycin- and control-treated subpools), we tabulated the $\log_2$ ratio of the normalized abundance in the control sample divided by the normalized abundance in the tunicamycin-treatment sample, which we call the tunicamycin effect on the respective transposon mutant as detected by RH-seq. In formulating this ratio, we assigned a pseudocount of 1 for each case of an insertion with zero reads in either the tunicamycin-treated or control sample of its respective round. For insertions detected in multiple rounds, we averaged the tunicamycin effect across all rounds before proceeding. For a given gene, we compiled all transposon insertion mutants in the gene as observed across all RH-seq rounds, and we used a two-sample Wilcoxon test to compare the tunicamycin effects between two sets of mutants: those in the N2 allele of the respective gene and those in the ED3077 allele. We corrected for multiple testing using the Benjamini-Hochberg method.

Generating Cas9 mutants of *cutl-24*

CRISPR-mediated genome editing was performed as described (Friedland *et al.* 2013) with modifications as follows. Purebred N2 and, separately, ED3077 as day 1 adult animals were injected with pDD162 (P*eft-3::Cas9::tbb-2utr*), pCFJ90 (P*myo-2::mCherry*) and two different pU6::sgRNAs targeting *cutl-24*. Surviving worms were separated, and F1 mCherry-positive animals were collected; their progeny, representing the F2 generation, were genotyped for the *cutl-24* gene. Mutant genotypes are reported in Supplementary Table 4.

***cutl-24* expression analysis**

For Figure 6, the *cutl-24* expression pattern was obtained from (Dillman *et al.* 2015; Hashimshony *et al.* 2015). For Figure 7, the *cutl-24* expression pattern in single cell resolution was obtained from (Packer *et al.* 2019). Cell type labels follow the format CellType:StartTime_EndTime, where times represent development following fertilization: ILso, Inner labial socket; AMso, Amphid socket; CEPsh, Cephalic sheath; CEPso, Cephalic socket; ADEsh, Anterior dereid sheath; PHB_and_possibly_PHA, PHB/PHA neuron;

ILsh_OLLsh_OLQsh, Inner/outer labial sheath; XXX, Glia and excretory cells; ASG, ADL, AWA, ASH and ADE, neurons of other types; AMso_PHso, Amphid and phasmid socket; ADE_CEP_PDE, neurons.

Code availability

Custom Python and R scripts used for RH-seq data analysis are available at https://github.com/annagflury/RHseq-scripts.

Data availability

RH-seq data have been deposited in the Sequence Read Archive (SRA), submission ID SUB9564728.

Results

Tunicamycin resistance in wild *C. elegans* and its parent-of-origin dependence

Tunicamycin, a N-glycosylation inhibitor and ER stress inducer, causes developmental delay in nematodes (Richardson *et al.* 2011). To identify *C. elegans* strains resistant to this defect, we collected eggs from each of a panel of wild isolates and the laboratory strain N2, exposed them to a toxic concentration of tunicamycin, and tabulated the number of successfully developed adults after 96 hours at 20°C. Among these strains, the predominant phenotype was of marked sensitivity, in which most eggs exposed to tunicamycin failed to reach adulthood, and indeed never reached the larval stage of development (Figure 1). All isolates we assayed fit this description except one: ED3077, originally isolated from a park in Nairobi, Kenya, had a rate of development in the presence of the drug outstripping that of the rest of the panel by >2-fold (Figure 1). We targeted this tunicamycin resistance phenotype in ED3077 as a compelling target

for genetic dissection, and we chose to use N2 as a representative of the tunicamycin-sensitive state.

To begin to investigate the genetics of tunicamycin resistance in ED3077, we mated this strain to N2, and subjected the resulting F1 hybrid eggs to our tunicamycin development assay. Results made clear that the hybrid phenotype depended on the direction of the cross (Figure 2). ED3077 hermaphrodites, mated to N2 males, yielded eggs that developed in tunicamycin conditions at a rate approaching that of the ED3077 purebred. By contrast, hybrids with N2 as the hermaphrodite parent had almost no ability to develop in the presence of tunicamycin (Figure 2). Thus, the ED3077 phenotype was partially dominant over that of N2, but only when ED3077 was the hermaphrodite in the cross. We hypothesized that the mechanism of this maternal effect could bear on the genetics of the trait difference between purebred ED3077 and N2. In what follows, we describe our experiments to probe both facets of the system.

RH-seq reveals allelic effects of *cutl-24* in an inter-strain hybrid

We sought to identify the genetic basis of the parent-of-origin-dependent tunicamycin resistance trait in the ED3077 x N2 system using RH-seq. The method requires large cohorts of hybrids harboring disrupting mutations in one of the two copies of each gene in turn, and we chose the Mos1 transposon system (Bessereau *et al.* 2001; Williams *et al.* 2005) for this purpose. We set up a workflow to generate transposon mutants in ED3077 or N2 and mate each to the wild-type of the respective other parent, yielding hemizygote eggs (Figure 3). In each case we used hermaphrodites as the transposon mutant parent and males as the wild-type, in light of the importance of the hermaphrodite genotype in hybrids (Figure 2). We incubated hemizygote eggs in tunicamycin or untreated control conditions, and then collected animals that reached adulthood for DNA isolation and sequencing.

We reasoned that deploying this RH-seq setup at moderate scale could reveal candidate determinants of tunicamycin resistance in the ED3077 x N2 hybrid. To this end, we generated

and detected a total of 74,893 hemizygote genotypes from DNAs of animals reaching adulthood in tunicamycin and in control conditions, after quality-control filtering of sequencing data (Supplementary Tables 1 and 2). Focusing on the 2,722 highest-coverage genes, we tested for a difference in normalized sequencing representation among tunicamycin-treated adults between two cohorts of hemizygotes—those with the ED3077 allele uncovered and those with the N2 allele uncovered. In this test, several genes exhibited suggestive evidence for allelic effects unique to tunicamycin resistance, though none reached significance after correction for multiple testing (Supplementary Table 3). We considered each such gene to represent a potential candidate determinant of tunicamycin response, whose *bona fide* function could be validated in single-gene experimental follow-up.

Manual inspection pointed to *cutl-24*, encoding a largely uncharacterized protein containing a cuticlin-like domain, as a candidate of particular interest on the basis of the robust potential impact of allelic variation (Figure 4). In RH-seq data, genotypes with the ED3077 allele disrupted in the hybrid, leaving the N2 uncovered and functional, were at low abundance in tunicamycin-treated adults relative to controls; genotypes with the ED3077 allele intact and the N2 allele disrupted were abundant in these samples (Figure 4). On this basis we hypothesized that the ED3077 allele of *cutl-24* had pro-resistance activity in the hybrid, to an extent greater than the effects of the N2 allele.

***cutl-24* as a determinant of tunicamycin resistance in hybrids and purebreds**

To validate the role of *cutl-24* in trait variation in the ED3077 x N2 system, we first focused on the hybrid background, where this gene had been a top scorer in our RH-seq screen. We used Cas9 to generate stable lines of purebred N2 and ED3077 harboring a nonsense mutation in *cutl-24* (Supplementary Table 4). We mated each mutant as the hermaphrodite to the respective wild-type male of the other strain, as in our RH-seq setup (Figures 3-4), and we subjected the progeny to development assays in the presence of tunicamycin. The results showed that

disrupting *cutl-24* in ED3077 hermaphrodites, followed by crossing to wild-type male N2, compromised tunicamycin resistance of the hybrid by >2-fold (Figure 5a), consistent with the trend we had observed in RH-seq (Figure 4). Mutating *cutl-24* in N2 hermaphrodites, followed by mating with wild-type ED3077 males, had no such effect and instead appeared to confer a benefit in the hybrid (though this trend was not significant; Figure 5a). These data establish *cutl-24* as a driver of the unique tunicamycin resistance phenotype of the hybrid progeny of ED3077 hermaphrodites, and serve as a validation of the RH-seq approach.

We also examined the importance of *cutl-24* in the male parent of inter-strain hybrids. *cutl-24* mutation in ED3077 males conferred only a slight, non-significant drop in tunicamycin resistance of their hybrid progeny, in matings with N2 hermaphrodites; the same was true when N2 mutants were the male parent of a cross with ED3077 hermaphrodites (Figure 5b). That is, *cutl-24* mutation in males had little if any impact on hybrid tunicamycin response, regardless of background. This result echoed our finding from wild-type crosses that hermaphrodite genotype matters most for tunicamycin resistance in hybrids (Figure 2). Together, our genetic analyses establish *cutl-24* as a determinant of the parent-of-origin-dependent tunicamycin resistance in ED3077 x N2 hybrids, with the ED3077 allele in the hermaphrodite sufficient to explain the hybrid resistance phenotype entirely.

We hypothesized that *cutl-24* could also contribute to tunicamycin resistance in a purebred context. As expected, the N2 purebred performed so poorly in tunicamycin resistance assays that *cutl-24* mutation effects could not be resolved (Figure 5c). Such a detection floor in the assay signal was not an issue for purebred ED3077, in which we observed a 20% drop in tunicamycin resistance in the *cutl-24* mutant relative to wild-type (Figure 5c). This modest but significant phenotype was much less dramatic than the impact of *cutl-24* mutation we had detected in hybrids (Figure 5a). Such a contrast points up the behavior of the hybrid as a sensitized background, in which *cutl-24* dependence is amplified and drives striking parent-of-

origin effects (Figure 5a-b). In purebred ED3077, we infer that *cutl-24* acts instead as a modifier of tunicamycin resistance, likely one of many determinants of a complex genetic architecture.

Evidence for *cutl-24* as a neuronal factor

To help formulate models for *cutl-24* activity and function, we characterized the localization of its gene product with an expression analysis approach. In whole-worm developmental timecourses (Dillman *et al.* 2015; Hashimshony *et al.* 2015), *cutl-24* expression was high in embryos and lower but appreciable in larvae and adults (Figure 6). Lineage-traced single-cell transcriptomes through development (Packer *et al.* 2019) found *cutl-24* in glia of the inner labial sensilla and, at lower levels, in many other neurons (Figure 7). In adult hermaphrodites, RNA tagging for a marker of outer labial sensilla neurons and PVD nociceptors revealed significant *cutl-24* expression (Smith *et al.* 2010). These results establish the presence of the *cutl-24* gene product in a range of neuronal cells, and raise the possibility that *cutl-24* may exert its effect on development and stress resistance in this context.

Discussion

The search for genes underlying natural trait variation has been a mandate for geneticists since Mendel. Wild nematodes have great potential as a study system for ecological genetics (Frézal and Félix 2015; Cook *et al.* 2017). In these animals, landmark studies have identified variants with Mendelian (de Bono and Bargmann 1998; Reddy *et al.* 2009; McGrath *et al.* 2009; Bendesky *et al.* 2012; Ghosh *et al.* 2012, 2015; Balla *et al.* 2015; Large *et al.* 2016) and maternal-effect (Ben-David *et al.* 2017; Ewe *et al.* 2020) modes of action that underlie phenotypes of interest. Many of these successes have derived from model advanced intercross mapping populations in *C. elegans* (Li *et al.* 2006; Rockman and Kruglyak 2009; Doroszuk *et al.* 2009; Andersen *et al.* 2015). In non-model nematode strains and species, statistical genetics

continues to pose challenges, owing to population structure among wild isolates (Webster *et al.* 2019b) and low meiotic recombination rates in lab crosses (Hillers and Villeneuve 2003).

In this work, we have established strain differences and parent-of-origin effects in worm ER stress resistance. And we have used a new tool, RH-seq, alongside classical genetics to identify *cutl-24* as a determinant of the variation. By discovering maternal-effect and development-related functions of this uncharacterized gene, our study underscores the utility of the natural variation approach, and RH-seq in particular, in nematodes.

The RH-seq approach in *C. elegans*

RH-seq shares with several other worm screening methods (Frézal *et al.* 2018; Burga *et al.* 2019; Webster *et al.* 2019b) the ability to streamline phenotyping assays by bulk sequencing of naturally varying strains. The chief distinction of RH-seq is its ability to map genotype to phenotype without recombinant progeny from crosses, in the lab or in the wild (Weiss *et al.* 2018; Weiss and Brem 2019). As such, here the technique has enabled genetic dissection in non-model *C. elegans* ED3077 in the absence of a panel of recombinant inbred lines. More broadly, the utility of RH-seq for any worm strains or species will be a function of mutagenesis throughput and phenotyping signal-to-noise, which will govern coverage and statistical power in a given implementation. Our mapping of *cutl-24* in a screen of limited depth and power serves as a compelling demonstration of the method.

Maternal effects of strain variation and *cutl-24* function

Starting from the discovery of a unique tunicamycin resistance phenotype in the Kenyan *C. elegans* isolate ED3077, we found that ED3077 x N2 hybrid embryos develop best in tunicamycin when they arise from ED3077 hermaphrodite parents rather than ED3077 males. Furthermore, these hybrid embryos rely on parent *cutl-24* far more than do ED3077 purebreds, under tunicamycin treatment. It is tempting to speculate that hybrids act as a sensitized

background for *cutl-24* mutation owing to stresses from genome incompatibility, as has been documented in other *C. elegans* crosses (Dolgin *et al.* 2007; Snoek *et al.* 2014). If so, hermaphrodite *cutl-24* could help maintain homeostasis under this burden, when compounded by tunicamycin.

Our work leaves open the mechanism by which *cutl-24* in hermaphrodites affects developing progeny. Given its expression in multiple neuronal types, *cutl-24* could participate in the newly described pathway linking neuronal serotonin in mothers with stress-protective transcription in their progeny (Das *et al.* 2020). Alternatively, acting in labial sensilla in particular, *cutl-24* could follow the precedent from other maternal-effect genes that directly modulate egg-laying and egg structure in the worm (Daniele *et al.* 2020; Min *et al.* 2020; Baugh and Hu 2020). Or *cutl-24* transcripts could be expressed in the germline and maternally deposited in the embryo for activity early in development, as is the case for other well-characterized maternal-effect factors (Robertson and Lin 2015).

In any such case, ED3077 hermaphrodites, reared under standard conditions in our assay design, would lay eggs better equipped to handle environmental and/or genetic challenges, in part mediated by *cutl-24*. Consistent with this notion, in a previous study of wild *C. elegans*, the ED3077 strain was distinguished by a marked ability for L1 larvae to develop successfully after starvation (Webster *et al.* 2019b). The emerging picture is one of a unique, broad stress-resistant phenotype in this isolate. Further work will establish its complete genetic architecture and the evolutionary forces that drove its appearance in the wild.

References

Andersen E. C., T. C. Shimko, J. R. Crissman, R. Ghosh, J. S. Bloom, *et al.*, 2015 A Powerful New Quantitative Genetics Platform, Combining Caenorhabditis elegans High-Throughput Fitness Assays with a Large Collection of Recombinant Strains. G3 (Bethesda). 5: 911–920. https://doi.org/10.1534/g3.115.017178

Balla K. M., E. C. Andersen, L. Kruglyak, and E. R. Troemel, 2015 A wild C. elegans strain has enhanced epithelial immunity to a natural microsporidian parasite. PLoS Pathog. 11: e1004583. https://doi.org/10.1371/journal.ppat.1004583

Baugh L. R., and P. J. Hu, 2020 Starvation Responses Throughout the Caenorhabditis elegans Life Cycle. Genetics 216: 837–878. https://doi.org/10.1534/genetics.120.303565

Ben-David E., A. Burga, and L. Kruglyak, 2017 A maternal-effect selfish genetic element in Caenorhabditis elegans. Science 356: 1051–1055. https://doi.org/10.1126/science.aan0621

Bendesky A., J. Pitts, M. V Rockman, W. C. Chen, M.-W. Tan, *et al.*, 2012 Long-range regulatory polymorphisms affecting a GABA receptor constitute a quantitative trait locus (QTL) for social behavior in Caenorhabditis elegans. PLoS Genet. 8: e1003157. https://doi.org/10.1371/journal.pgen.1003157

Bessereau J. L., A. Wright, D. C. Williams, K. Schuske, M. W. Davis, *et al.*, 2001 Mobilization of a Drosophila transposon in the Caenorhabditis elegans germ line. Nature 413: 70–74. https://doi.org/10.1038/35092567

Bono M. de, and C. I. Bargmann, 1998 Natural variation in a neuropeptide Y receptor homolog modifies social behavior and food response in C. elegans. Cell 94: 679–689. https://doi.org/10.1016/s0092-8674(00)81609-8

Boulin T., and J. L. Bessereau, 2007 Mos1-mediated insertional mutagenesis in Caenorhabditis elegans. Nat. Protoc. 2: 1276–1287. https://doi.org/10.1038/nprot.2007.192

Burga A., E. Ben-David, T. Lemus Vergara, J. Boocock, and L. Kruglyak, 2019 Fast genetic mapping of complex traits in C. elegans using millions of individuals in bulk. Nat. Commun. 10: 2680. https://doi.org/10.1038/s41467-019-10636-9

Comings D. E., and J. P. MacMurray, 2000 Molecular heterosis: a review. Mol. Genet. Metab. 71: 19–31. https://doi.org/10.1006/mgme.2000.3015

Cook D. E., S. Zdraljevic, J. P. Roberts, and E. C. Andersen, 2017 CeNDR, the Caenorhabditis elegans natural diversity resource. Nucleic Acids Res. 45: D650–D657. https://doi.org/10.1093/nar/gkw893

Daniele J. R., R. Higuchi-Sanabria, J. Durieux, S. Monshietehadi, V. Ramachandran, *et al.*, 2020 UPR(ER) promotes lipophagy independent of chaperones to extend life span. Sci. Adv. 6: eaaz1441. https://doi.org/10.1126/sciadv.aaz1441

Das S., F. K. Ooi, J. Cruz Corchado, L. C. Fuller, J. A. Weiner, *et al.*, 2020 Serotonin signaling by maternal neurons upon stress ensures progeny survival. Elife 9. https://doi.org/10.7554/eLife.55246

Dillman A. R., M. Macchietto, C. F. Porter, A. Rogers, B. Williams, *et al.*, 2015 Comparative genomics of Steinernema reveals deeply conserved gene regulatory networks. Genome Biol. 16: 9–11. https://doi.org/10.1186/s13059-015-0746-6

Dolgin E. S., B. Charlesworth, S. E. Baird, and A. D. Cutter, 2007 Inbreeding and outbreeding depression in Caenorhabditis nematodes. Evolution 61: 1339–1352. https://doi.org/10.1111/j.1558-5646.2007.00118.x

Doroszuk A., L. B. Snoek, E. Fradin, J. Riksen, and J. Kammenga, 2009 A genome-wide library of CB4856/N2 introgression lines of Caenorhabditis elegans. Nucleic Acids Res. 37: e110.

https://doi.org/10.1093/nar/gkp528

Duverger Y., J. Belougne, S. Scaglione, D. Brandli, C. Beclin, *et al.*, 2007 A semi-automated high-throughput approach to the generation of transposon insertion mutants in the nematode Caenorhabditis elegans. Nucleic Acids Res. 35: 1–8. https://doi.org/10.1093/nar/gkl1046

Evansid K. S., J. Witid, L. Stevensid, S. R. Hahnel, B. Rodriguezid, *et al.*, 2021 Two novel loci underlie natural differences in Caenorhabditis elegans abamectin responses. PLoS Pathog. 17: 1–26. https://doi.org/10.1371/journal.ppat.1009297

Ewe C. K., Y. N. Torres Cleuren, S. E. Flowers, G. Alok, R. G. Snell, *et al.*, 2020 Natural cryptic variation in epigenetic modulation of an embryonic gene regulatory network. Proc. Natl. Acad. Sci. U. S. A. 117: 13637–13646. https://doi.org/10.1073/pnas.1920343117

Flint J., and R. Mott, 2001 Finding the molecular basis of quantitative traits: Successes and pitfalls. Nat. Rev. Genet. 2: 437–445. https://doi.org/10.1038/35076585

Frézal L., and M. A. Félix, 2015 C. elegans outside the Petri dish. Elife 4: 1–14. https://doi.org/10.7554/eLife.05849

Frézal L., E. Demoinet, C. Braendle, E. Miska, and M.-A. Félix, 2018 Natural Genetic Variation in a Multigenerational Phenotype in C. elegans. Curr. Biol. 28: 2588-2596.e8. https://doi.org/10.1016/j.cub.2018.05.091

Friedland A. E., Y. B. Tzur, K. M. Esvelt, M. P. Colaiácovo, G. M. Church, *et al.*, 2013 Heritable genome editing in C. elegans via a CRISPR-Cas9 system. Nat. Methods 10: 741–743. https://doi.org/10.1038/nmeth.2532

Ghosh R., E. C. Andersen, J. A. Shapiro, J. P. Gerke, and L. Kruglyak, 2012 Natural variation in a chloride channel subunit confers avermectin resistance in C. elegans. Science 335: 574–578. https://doi.org/10.1126/science.1214318

Ghosh R., J. S. Bloom, A. Mohammadi, M. E. Schumer, P. Andolfatto, *et al.*, 2015 Genetics of Intraspecies Variation in Avoidance Behavior Induced by a Thermal Stimulus in Caenorhabditis elegans. Genetics 200: 1327–1339. https://doi.org/10.1534/genetics.115.178491

Hashimshony T., M. Feder, M. Levin, B. K. Hall, and I. Yanai, 2015 Spatiotemporal transcriptomics reveals the evolutionary history of the endoderm germ layer. Nature 519: 219–222. https://doi.org/10.1038/nature13996

Hebert D. N., and M. Molinari, 2007 In and out of the ER: Protein folding, quality control, degradation, and related human diseases. Physiol. Rev. 87: 1377–1408. https://doi.org/10.1152/physrev.00050.2006

Henis-Korenblit S., P. Zhang, M. Hansen, M. McCormick, S.-J. Lee, *et al.*, 2010 Insulin/IGF-1 signaling mutants reprogram ER stress response regulators to promote longevity. Proc. Natl. Acad. Sci. 107: 9730 LP – 9735. https://doi.org/10.1073/pnas.1002575107

Hillers K. J., and A. M. Villeneuve, 2003 Chromosome-wide control of meiotic crossing over in C. elegans. Curr. Biol. 13: 1641–1647.

Large E. E., W. Xu, Y. Zhao, S. C. Brady, L. Long, *et al.*, 2016 Selection on a Subunit of the NURF Chromatin Remodeler Modifies Life History Traits in a Domesticated Strain of Caenorhabditis elegans. PLoS Genet. 12: e1006219. https://doi.org/10.1371/journal.pgen.1006219

Li Y., O. A. Alvarez, E. W. Gutteling, M. Tijsterman, J. Fu, *et al.*, 2006 Mapping determinants of gene expression plasticity by genetical genomics in C. elegans. PLoS Genet. 2: e222. https://doi.org/10.1371/journal.pgen.0020222

McGrath P. T., M. V Rockman, M. Zimmer, H. Jang, E. Z. Macosko, *et al.*, 2009 Quantitative mapping of a digenic behavioral trait implicates globin variation in C. elegans sensory

behaviors. Neuron 61: 692–699. https://doi.org/10.1016/j.neuron.2009.02.012

Min H., E. Youn, and Y.-H. Shim, 2020 Maternal Caffeine Intake Disrupts Eggshell Integrity and Retards Larval Development by Reducing Yolk Production in a Caenorhabditis elegans Model. Nutrients 12. https://doi.org/10.3390/nu12051334

Monk D., D. J. G. Mackay, T. Eggermann, E. R. Maher, and A. Riccio, 2019 Genomic imprinting disorders: lessons on how genome, epigenome and environment interact. Nat. Rev. Genet. 20: 235–248. https://doi.org/10.1038/s41576-018-0092-0

Na H., S. Zdraljevic, R. E. Tanny, A. J. M. Walhout, and E. C. Andersen, 2020 Natural variation in a glucuronosyltransferase modulates propionate sensitivity in a C. elegans propionic acidemia model. PLoS Genet. 16: 1–20. https://doi.org/10.1371/JOURNAL.PGEN.1008984

Nigon V. M., and M.-A. Félix, 2017 History of research on C. elegans and other free-living nematodes as model organisms. WormBook 2017: 1–84. https://doi.org/10.1895/wormbook.1.181.1

Packer J. S., Q. Zhu, C. Huynh, P. Sivaramakrishnan, E. Preston, *et al.*, 2019 A lineage-resolved molecular atlas of C. Elegans embryogenesis at single-cell resolution. Science (80-.). 365. https://doi.org/10.1126/science.aax1971

Reddy K. C., E. C. Andersen, L. Kruglyak, and D. H. Kim, 2009 A polymorphism in npr-1 is a behavioral determinant of pathogen susceptibility in C. elegans. Science 323: 382–384. https://doi.org/10.1126/science.1166527

Reinhold K., 2002 Maternal effects and the evolution of behavioral and morphological characters: A literature review indicates the importance of extended maternal care. J. Hered. 93: 400–405. https://doi.org/10.1093/jhered/93.6.400

Richardson C. E., S. Kinkel, and D. H. Kim, 2011 Physiological IRE-1-XBP-1 and PEK-1 signaling in Caenorhabditis elegans larval development and immunity. PLoS Genet. 7:

e1002391. https://doi.org/10.1371/journal.pgen.1002391

Robertson S., and R. Lin, 2015 The Maternal-to-Zygotic Transition in C. elegans. Curr. Top. Dev. Biol. 113: 1–42. https://doi.org/10.1016/bs.ctdb.2015.06.001

Rockman M. V, and L. Kruglyak, 2009 Recombinational landscape and population genomics of Caenorhabditis elegans. PLoS Genet. 5: e1000419. https://doi.org/10.1371/journal.pgen.1000419

Roth J., C. Zuber, S. Park, I. Jang, Y. Lee, *et al.*, 2010 Protein N-glycosylation, protein folding, and protein quality control. Mol. Cells 30: 497–506. https://doi.org/10.1007/s10059-010-0159-z

Seidel H. S., M. Ailion, J. Li, A. van Oudenaarden, M. V Rockman, *et al.*, 2011 A novel sperm-delivered toxin causes late-stage embryo lethality and transmission ratio distortion in C. elegans. PLoS Biol. 9: e1001115. https://doi.org/10.1371/journal.pbio.1001115

Smith C. J., J. D. Watson, W. C. Spencer, T. O'Brien, B. Cha, *et al.*, 2010 Time-lapse imaging and cell-specific expression profiling reveal dynamic branching and molecular determinants of a multi-dendritic nociceptor in C. elegans. Dev. Biol. 345: 18–33. https://doi.org/10.1016/j.ydbio.2010.05.502

Snoek L. B., H. E. Orbidans, J. J. Stastna, A. Aartse, M. Rodriguez, *et al.*, 2014 Widespread genomic incompatibilities in Caenorhabditis elegans. G3 (Bethesda). 4: 1813–1823. https://doi.org/10.1534/g3.114.013151

Stern D. L., 2014 Identification of loci that cause phenotypic variation in diverse species with the reciprocal hemizygosity test. Trends Genet. 30: 547–554. https://doi.org/10.1016/j.tig.2014.09.006

Timberlake W. E., 2013 Heterosis, pp. 451–453 in *Brenner's Encyclopedia of Genetics (Second Edition)*, edited by Maloy S., Hughes K. Academic Press, San Diego.

Webster A. K., A. Hung, B. T. Moore, R. Guzman, J. M. Jordan, *et al.*, 2019a Population Selection and Sequencing of Caenorhabditis elegans Wild Isolates Identifies a Region on Chromosome III Affecting Starvation Resistance. G3 Genes, Genomes, Genet. 9: 3477–3488. https://doi.org/10.1534/g3.119.400617

Webster A. K., A. Hung, B. T. Moore, R. Guzman, J. M. Jordan, *et al.*, 2019b Population Selection and Sequencing of Caenorhabditis elegans Wild Isolates Identifies a Region on Chromosome III Affecting Starvation Resistance. G3 (Bethesda). 9: 3477–3488. https://doi.org/10.1534/g3.119.400617

Weiss C. V, J. I. Roop, R. K. Hackley, J. N. Chuong, I. V Grigoriev, *et al.*, 2018 Genetic dissection of interspecific differences in yeast thermotolerance. Nat. Genet. 50: 1501–1504. https://doi.org/10.1038/s41588-018-0243-4

Weiss C. V, and R. B. Brem, 2019 Dissecting Trait Variation across Species Barriers. Trends Ecol. Evol. 34: 1131–1136. https://doi.org/10.1016/j.tree.2019.07.013

Williams D. C., T. Boulin, A. F. Ruaud, E. M. Jorgensen, and J. L. Bessereau, 2005 Characterization of Mos1-mediated mutagenesis in Caenorhabditis elegans: A method for the rapid identification of mutated genes. Genetics 169: 1779–1785. https://doi.org/10.1534/genetics.104.038265

Wolf J. B., and M. J. Wade, 2009 What are maternal effects (and what are they not)? Philos. Trans. R. Soc. B Biol. Sci. 364: 1107–1115. https://doi.org/10.1098/rstb.2008.0238

Figure captions

Figure 1. Tunicamycin resistance phenotypes of wild *C. elegans* isolates. The *y*-axis reports the proportion of eggs from the indicated wild isolate that developed to adulthood in the presence of tunicamycin. For a given column, each dot represents results from one replicate population, and the bar height reports the mean. ***, $p < 0.001$.

Figure 2. Tunicamycin resistance of inter-strain hybrids depends on the parent of origin. The *y*-axis reports the proportion of eggs from the indicated cross that developed to adulthood in the presence of tunicamycin, normalized to the analogous quantity from wild-type ED3077. For a given column, each dot represents results from one replicate population, and the bar height reports the mean. ED, ED3077; herm, hermaphrodite. **, $p < 0.01$.

Figure 3. Making hemizygote mutants for RH-seq. RH-seq requires hemizygote hybrids (purple) from matings between mutants of one background (red) and wild-types of another (blue). Top: arrays (circles) harboring the Mos1 transposon substrate (green) and heat-shock-inducible transposase enzyme gene (yellow) in the red background come together into one strain. Center: after heat shock, a transposon copy integrates into the genome (straight black line) of an egg of the red background, which is fertilized by a wild-type male of the blue background. Bottom: the resulting F1 hybrids are hemizygous throughout the soma and are used as input into a sequencing-based tunicamycin resistance assay.

Figure 4. RH-seq reveals *cutl-24* as a candidate gene at which allelic variation contributes to tunicamycin resistance. Each row reports results from a hemizygote mutant in which the Mos1 transposon has inserted into the N2 (a) or ED3077 (b) allele of *cutl-24* in the inter-strain F1 hybrid background. For a given row, the red triangle indicates the Mos1 insertion position in the *cutl-24* locus; the heat map reports the relative abundance of the hemizygote, as measured

by RH-seq, after tunicamycin selection as a difference from the analogous quantity from a control culture.

Figure 5. *cutl-24* in ED3077 mothers is required for tunicamycin resistance in their inter-strain hybrid progeny. Shown are tunicamycin resistance measurements in (a) F1 hybrids whose hermaphrodite parent of the indicated background harbored a mutation in *cutl-24,* and wild-type controls*;* (b) F1 hybrids whose male parent of the indicated background harbored a mutation in *cutl-24,* and wild-type controls*;* and (c) purebred *cutl-24* mutants and wild-type controls. In each panel, phenotype measurements were normalized to the analogous quantity from a wild-type ED3077 included in the experiment as a standard. For a given column, each dot represents results from one replicate population, and the bar height reports the mean. ED, ED3077; herm, hermaphrodite. *, $p < 0.05$; **, $p < 0.01$; n.s., not significant.

Figure 6. *cutl-24* expression across *C. elegans* developmental stages. In a given panel, each bar reports average expression (FPKM, Fragments Per Kilobase of transcript per Million mapped reads) of *cutl-24* in wild-type animals of the N2 background from (Dillman *et al.* 2015; Hashimshony *et al.* 2015). in the indicated developmental stage (a) or sex of adult animals (b). Error bars report standard deviation ($n = 2$).

Figure 7. *cutl-24* is expressed in neurons. In a given panel, each bar reports *cutl-24* expression (TPM, Transcripts Per Million kilobases) in the indicated cell type from single cell transcriptomes (Packer *et al.* 2019), in embryos at the indicated developmental time in minutes (a) or in L2 larvae (b). The highest expression was seen in inner labial socket (ILso), cephalic socket (CEPso), and phasmid socket (PHso) cells; for other abbreviations in labels, see Methods.

Supplementary table captions

Supplementary Table 1. RH-seq library sizes. Each row reports sequencing results from hemizygotes in the N2 x ED3077 diploid hybrid background, made from transposon mutants of the indicated strain mated to the wild-type of the other.

Supplementary Table 2. Abundance of hemizygote mutants in tunicamycin RH-seq. Abundances of transposon-mutant Mos1 insertion site in the F1 hybrid of N2 or ED3077 allele from RH-seq. Each row reports results of sequencing one transposon insertion in the N2 x ED3077b diploid hybrid after selection of the transposon mutant pool, reflecting the abundance in the pool of the respective hemizygote clone harboring the insertion. Gene, chromosome, and position report the fine-scale position of the insertion. Allele, the strain parent's homolog in which the transposon insertion lay. Control_count and treatment_count report read counts of the transposon insertion sequenced after selection of the mutant pool in the indicated condition, normalized for library size. Transposon insertions not detected in any replicate of the indicated selection were assigned an abundance of 1.

Supplementary Table 3. Effects of allelic variation in tunicamycin RH-seq. Each row reports the results of reciprocal hemizygote tests of tunicamycin resistance of hemizygote transposon mutants at the indicated gene in the N2 x ED3077 diploid hybrid. N2_control_count, N2_treatment_count, ED3077_control_count, and ED3077_treatment_count report normalized abundances of a hemizygote harboring a transposon insertion in the indicated parent's homolog after culture in the indicated condition, as a mean across transposon mutants, from all biological replicates. The last two columns report results of a two-tailed Mann-Whitney statistical test for a difference in the abundance after tunicamycin selection, relative to the abundance in an untreated control, of hemizygotes harboring transposon insertions in the two parents' homologs. The Benjamini-Hochberg method was used to correct for multiple testing.

Supplementary Table 4. *cutl-24* mutants. Each pair of rows reports the context of a Cas9-induced mutation (red) in the *cutl-24* gene of the indicated *C. elegans* strain. Uppercase, exonic sequence; lowercase, intronic sequence.

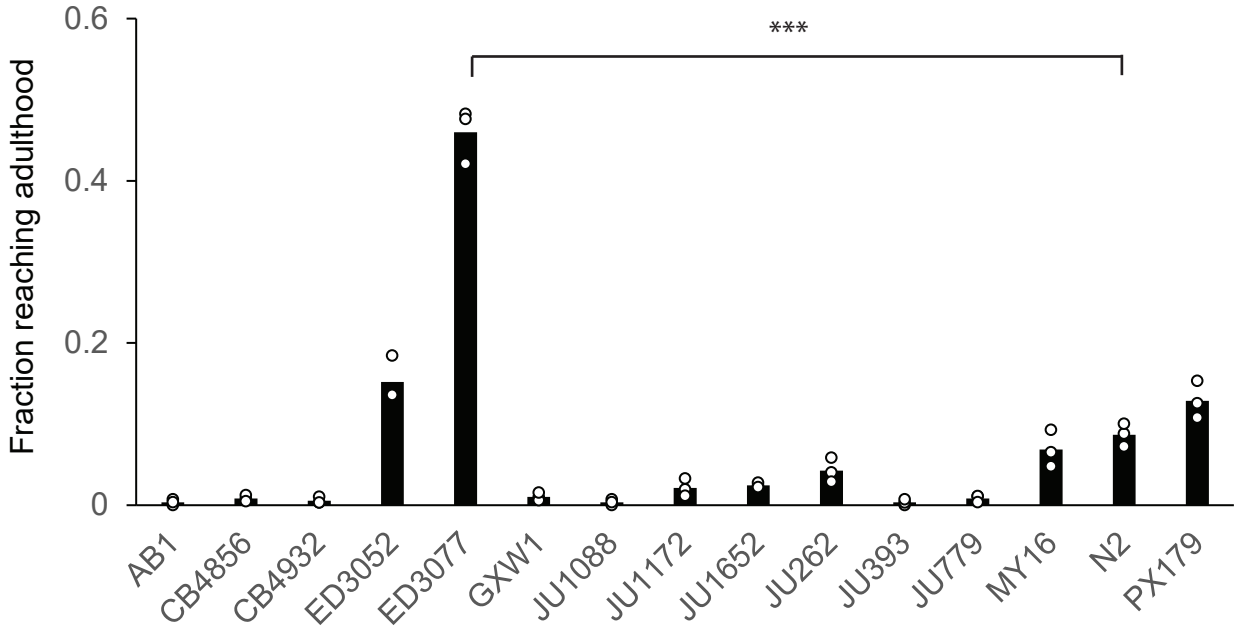
Fraction reaching adulthood
0.6
0.4
0.2
0
***
AB1
CB4856
CB4932
ED3052
ED3077
GXW1
JU1088
JU1172
JU1652
JU262
JU393
JU779
MY16
N2
PX179

Figure 1

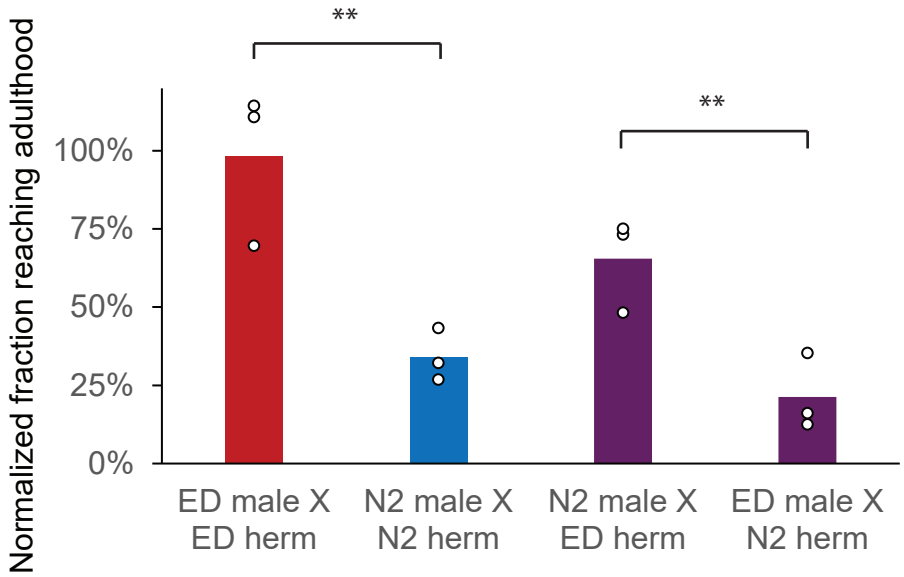
**
**
Normalized fraction reaching adulthood
100%
75%
50%
25%
0%
ED male X
ED herm
N2 male X
N2 herm
N2 male X
ED herm
ED male X
N2 herm

Figure 2

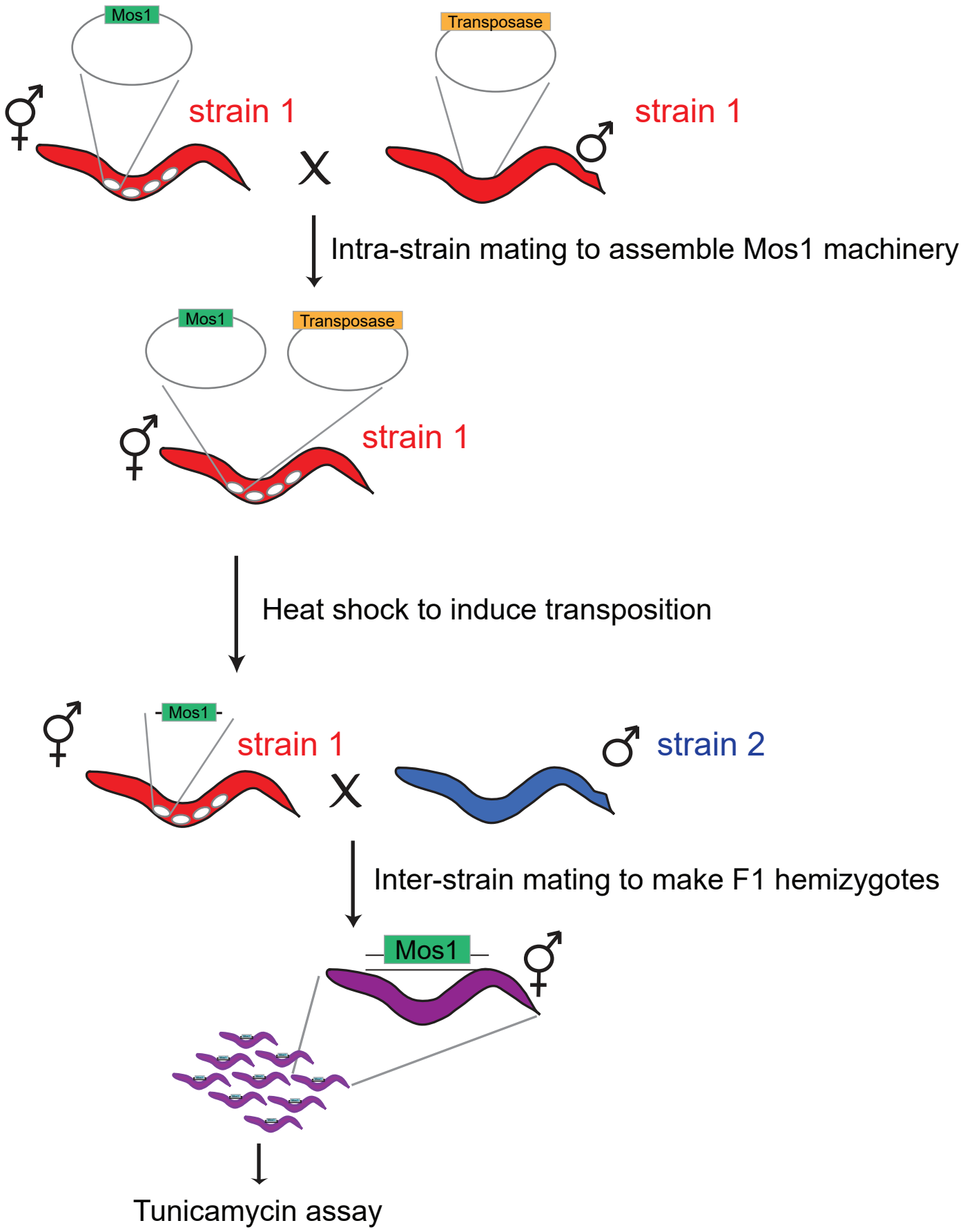
Mos1
strain 1
Transposase
strain 1
Intra-strain mating to assemble Mos1 machinery
Mos1
Transposase
strain 1
Heat shock to induce transposition
Mos1
strain 1
strain 2
Inter-strain mating to make F1 hemizygotes
Mos1
Tunicamycin assay

Figure 3

4a

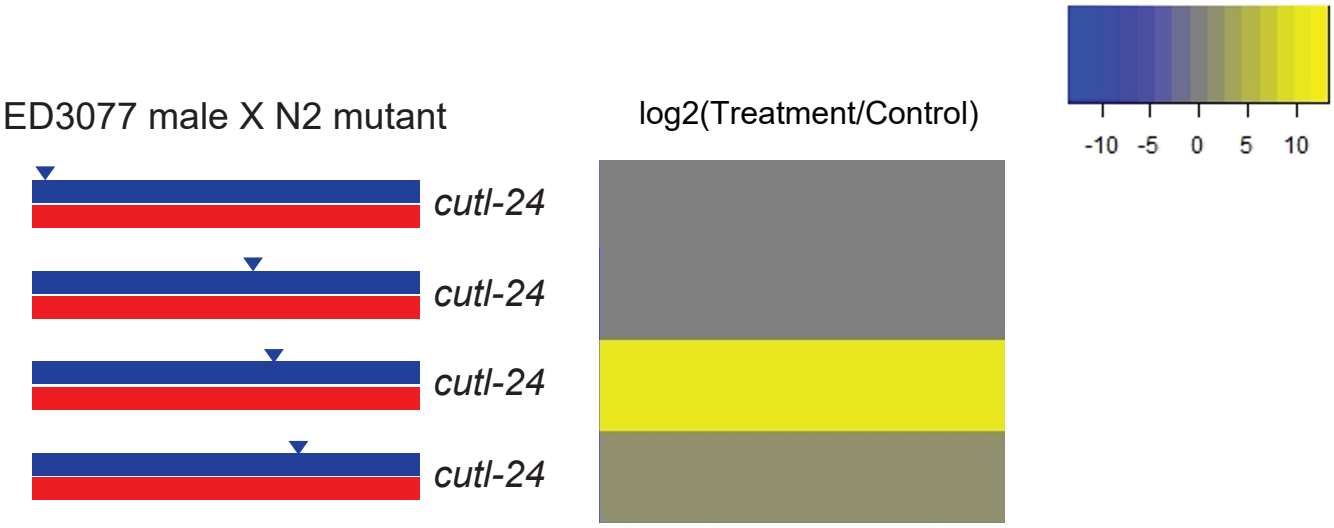

4b

Figure 4

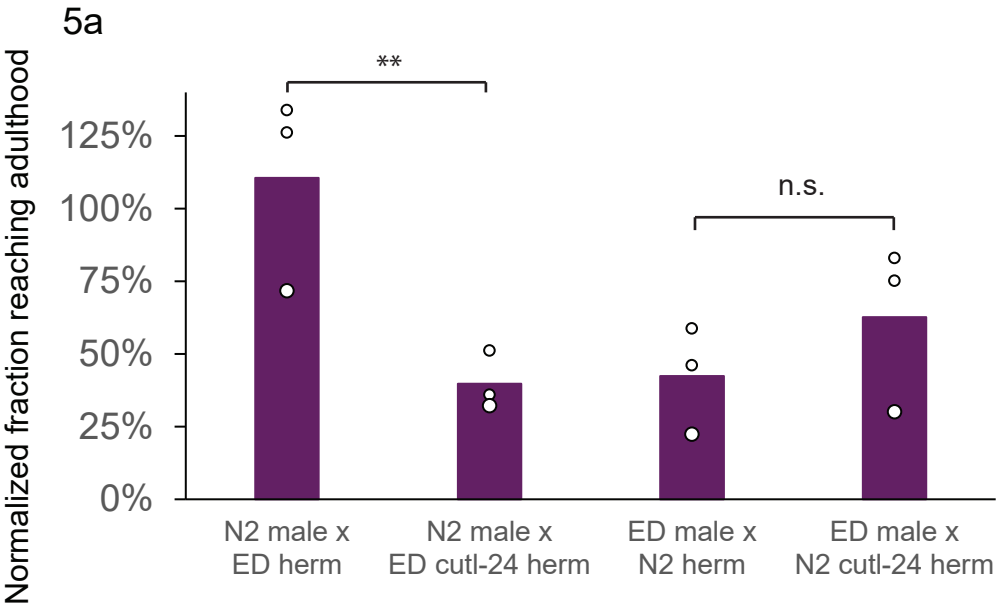
5a
Normalized fraction reaching adulthood
125%
100%
75%
50%
25%
0%
**
n.s.
N2 male x ED herm
N2 male x ED cutl-24 herm
ED male x N2 herm
ED male x N2 cutl-24 herm

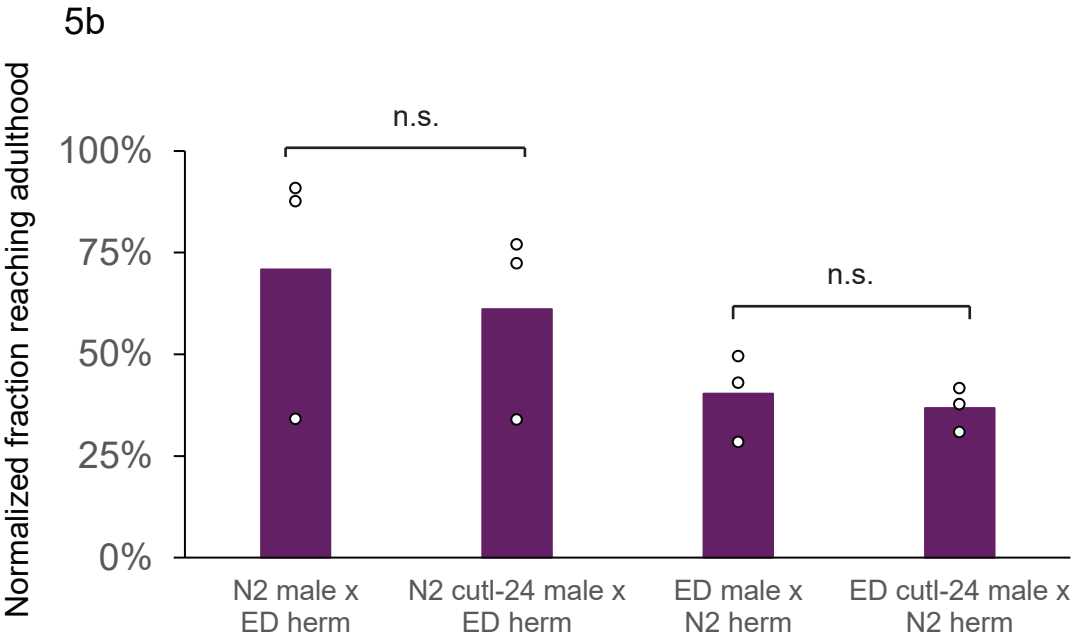
5b
Normalized fraction reaching adulthood
100%
75%
50%
25%
0%
n.s.
n.s.
N2 male x ED herm
N2 cutl-24 male x ED herm
ED male x N2 herm
ED cutl-24 male x N2 herm

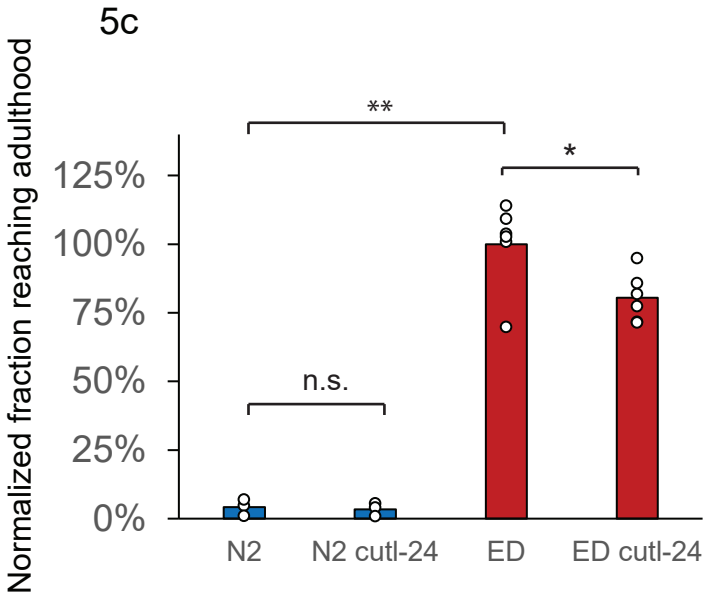
5c
Normalized fraction reaching adulthood
125%
100%
75%
50%
25%
0%
**
*
n.s.
N2
N2 cutl-24
ED
ED cutl-24

Figure 5

6a

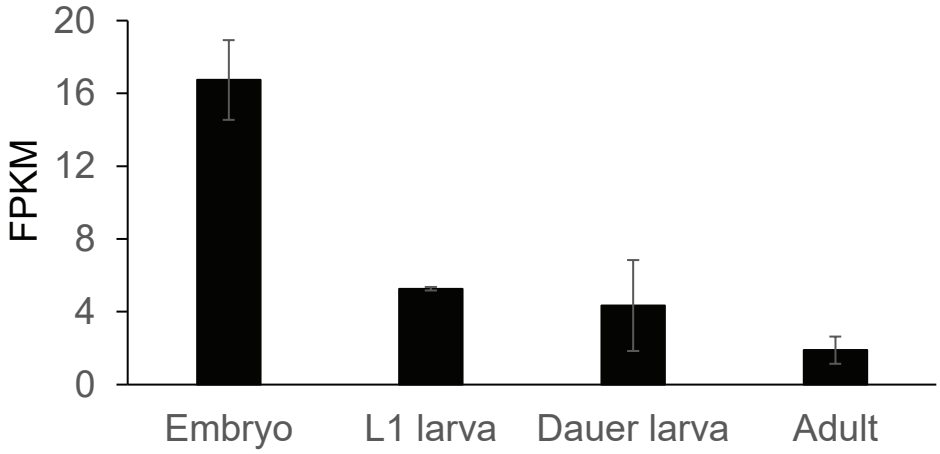

6b

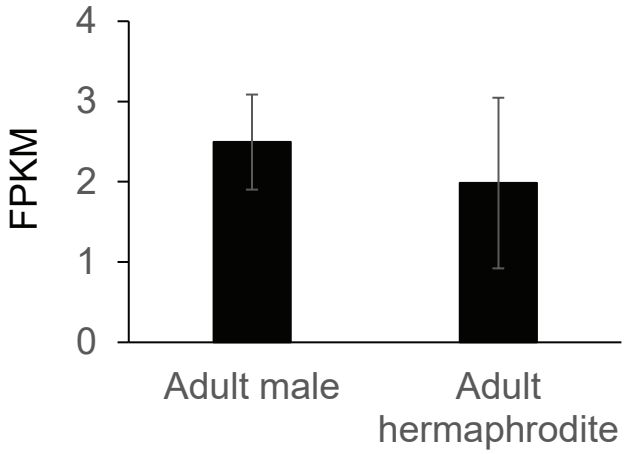

Figure 6

7a

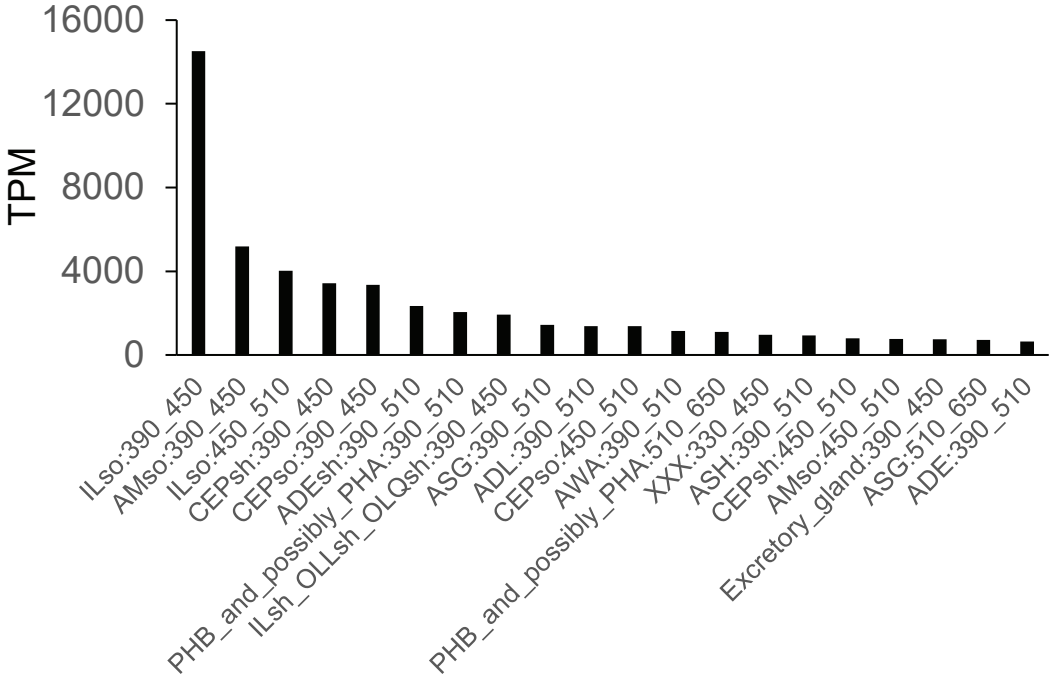

7b

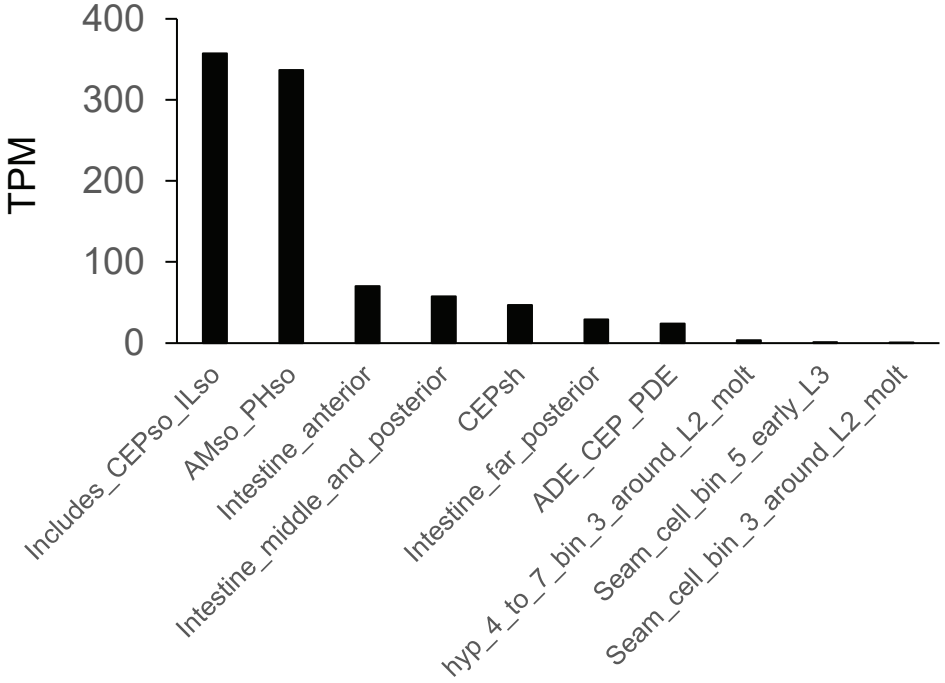

Figure 7